

Alkyl Complexes of Rare-Earth Metal Centers Supported by Chelating 1,1'-Diamidoferrocene Ligands: Synthesis, Structure, and Application in Methacrylate Polymerization

Jörg Eppinger,^{*,†} Katharina R. Nikolaides,[†] Mei Zhang-Prese,[†] Florian A. Riederer,[†]
Gerd W. Rabe,[†] and Arnold L. Rheingold[‡]

Department Chemie, Technische Universität München, Lichtenbergstrasse 4, D-85747 Garching, Germany,
and Department of Chemistry & Biochemistry, University of California,
San Diego, La Jolla, California 92093

Received October 3, 2007

Conversion of 1,1'-dianilinoferrocenes of the composition $[3,4-R_2C_5H_2(NHPh)]_2Fe$ ($R = H, Ph$) with 1 equiv of the rare-earth metal alkyl precursors $Ln(THF)_2(CH_2SiMe_3)_3$ ($Ln = Lu, Y$) affords $[R_4Fc(NPh)_2]Ln(THF)_2CH_2SiMe_3$ (**1a–2b**) in yields of 73–83%. The steric bulk of the ferrocene moiety induces a pronounced stabilization of the complexes in comparison to alkyl-bridged analogues. Correspondingly, the complexes **1a–2b** are stable in solution at room temperature and were characterized by multinuclear NMR spectroscopy and elemental analysis. A single-crystal X-ray diffraction study was performed for complex **2b**. The synthesized rare-earth metal alkyls embedded into a 1,1'-diamidoferrocene framework effectively initiate the polymerization of methyl methacrylate (MMA) at room temperature, producing isotactic enriched poly(methyl methacrylate) (PMMA). The properties of the produced PMMAs are mainly governed by the substitution patterns of the ferrocenyl backbone.

Introduction

Currently, electrophilic rare-earth metal centers supported by nitrogen-containing chelates are intensively explored as valuable catalysts for a variety of transformations.^{1–6} Termed “postmetallocenes”, they have proven to effectively promote polymerizations of cyclic esters² as well as a variety of olefin transformations, with hydroaminations³ and the polymerization of nonpolar⁴ or polar functionalized olefins^{5,6} being of particular interest. It is generally accepted that the reactivity of rare-earth metal complexes is driven by electrophilicity and coordinative unsaturation of the metal center, which can be controlled through tuning of the ancillary ligation.^{1,6} Surprisingly, despite their unique combination of steric and electronic properties, chelating ligands containing a ferrocenyl backbone have not been

introduced into rare-earth metal chemistry, so far.⁷ Here we report the first examples of rare-earth metal centers ligated by 1,1'-diamidoferrocenes and investigate the influence of the ferrocenyl unit on the reactivity of the corresponding alkyl complexes.

Results and Discussion

Adapting the synthetic route initially proposed by Anwander et al.,⁶ compounds **1a–2b** of the general composition $[R_4Fc(NPh)_2]Ln(THF)_2CH_2SiMe_3$ ($Ln = Y, Lu; R = H, Ph$) were readily accessible by deprotonation of the diamidoferrocene **L1** or **L2** with equimolar amounts of $Ln(THF)_2(CH_2SiMe_3)_3$ at ambient temperature (Scheme 1). The products are well soluble in arene solvents and can be precipitated in high purity as orange-red powders by addition of *n*-hexanes. A comparison with alkyl-bridged analogues reveals a surprisingly high stabilization by the ferrocenyl ligands. This fact underlines the exceptional steric properties of the ferrocenyl backbone. While the latter are stable for weeks at room temperature in toluene solution, the ethylene diamide complexes **3a–5b** decompose quickly under these conditions (Scheme 2). Only the

* Corresponding author. Fax: +49 89 289 13473. E-mail: joerg.eppinger@ch.tum.de.

[†] Technische Universität München.

[‡] University of California.

(1) (a) Zeimentz, P. M.; Arndt, S.; Elvidge, B. R.; Okuda, J. *Chem. Rev.* **2006**, *106*, 2404–2433. (b) Trifonov, A. A.; Skvortsov, G. G.; Lyubov, D. M.; Skorodumova, N. A.; Fukin, G. K.; Baranov, E. V.; Glushakova, V. N. *Chem.–Eur. J.* **2006**, *12*, 5320–5327. (c) Edlmann, F. T.; Freckmann, D. M. M.; Schumann, H. *Chem. Rev.* **2002**, *102*, 1851–1896. (d) Piers, W. E.; Emslie, D. J. H. *Coord. Chem. Rev.* **2002**, *233–234*, 131–155.

(2) (a) Yang, Y.; Li, S.; Cui, D.; Chen, X.; Jing, X. *Organometallics* **2007**, *26*, 671–678. (b) Gamer, M. T. P. W.; Roesky, P. W.; Palard, I.; Hellaye, M. L.; Guillaume, S. M. *Organometallics* **2007**, *26*, 651–657.

(3) (a) Rastätter, M.; Zuly, A.; Roesky, P. W. *Chem. Commun.* **2006**, 874–876. (b) Martínez, P. H.; Hultsch, K. C.; Hampel, F. *Chem. Commun.* **2006**, 2221–2223. (c) Meyer, N.; Zuly, A.; Roesky, P. W. *Organometallics* **2006**, *25*, 4179–4182.

(4) (a) Ge, S.; Bambirra, S.; Meetsma, A.; Hessen, B. *Chem. Commun.* **2006**, 3320–3322. (b) Kretschmer, W. P.; Meetsma, A.; Hessen, B.; Schmalz, T.; Qayyum, S.; Kempe, R. *Chem.–Eur. J.* **2006**, *12*, 8969–8978. (5) Chui, C.; Shafir, A.; Reeder, C. L.; Arnold, J. *Organometallics* **2003**, *22*, 3357–3359.

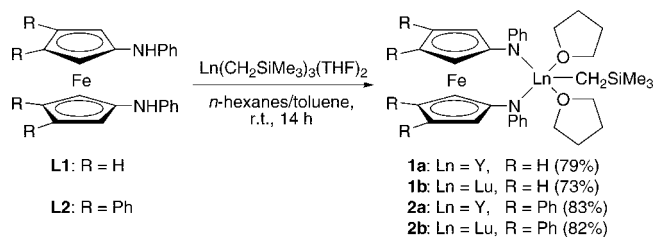
(6) Estler, F.; Eickerling, G.; Herdtweck, E.; Anwander, R. *Organometallics* **2003**, *22*, 1212–1222.

(7) (a) To the best of our knowledge, to date no complex of a rare-earth metal center chelated by a ligand with a ferrocenyl backbone has been published so far. However, several reports of rare-earth metal complexes with ferrocenyl moieties in the side chain of a ligand exist, e.g.: Baskar, V.; Roesky, P. W. *Dalton Trans.* **2006**, 676–679. (b) 1,1'-Diamidoferrocene complexes of group 4 metals have been highlighted recently: Herberhold, M. *Angew. Chem., Int. Ed.* **2002**, *41*, 956–958. (c) For the first example of a 1,1'-diamidoferrocene complexes of an actinide element see: Monreal, M. J.; Carver, T. C.; Diaconescu, P. L. *Inorg. Chem.* **2007**, *46*, 7226–7228.

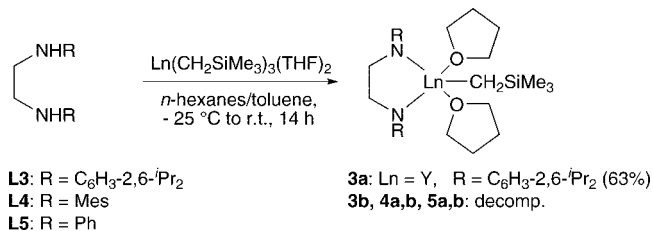
(8) Ligand synthesis is based on published procedures. (a) **L2**: Plenio, H.; Burth, D. *Organometallics* **1996**, *15*, 4054–4062. (b) **L1**: Siemeling, U.; Kuhnert, O.; Neumann, B.; Stammler, A.; Stammler, H.-G.; Bildstein, B.; Malaun, M.; Zanello, P. *Eur. J. Inorg. Chem.* **2001**, 913–916. (c) Siemeling, U.; Auch, T.-C.; Kuhnert, O.; Malaun, M.; Kopacka, H.; Bildstein, B. *Z. Anorg. Allg. Chem.* **2003**, *629*, 1334.

(9) Lappert, M. F.; Pearce, R. *Chem. Commun.* **1973**, 126–126.

Scheme 1. Synthesis of Complexes 1a–2b



Scheme 2. Synthesis of Complex 3a



2,6-diisopropylphenyl residue introduces sufficient steric shielding to stabilize the yttrium alkyl compound **3a** well enough to allow isolation and spectroscopic characterization. Chelates containing a Lu(III) center (**3b**) or the less bulky mesityl (**4a,b**) or phenyl (**5a,b**) substituents decompose rapidly, as observed frequently for alkyl complexes of rare-earth metal cations.^{6,10}

Spectroscopic and microanalytic data of compounds **1a–3a** are consistent with the formation of the bis(THF) adduct featuring a pentacoordinate metal center.¹¹ The ¹H NMR resonances of the neosilyl moiety show a relative downfield shift for the ferrocenyl complexes of up to 0.29 ppm compared to complex **3a** and of up to 0.96 ppm compared to analogous rare-earth metal alkyl complexes of chelating diamide ligands.^{5,6} This indicates that in solution the silyl moiety is preferably located in the deshielding cone of the anilide phenyl rings, an observation that is in agreement with the coplanar orientation of the arenes in the solid state structure (Figure 2).

Cyclic voltammetric studies in acetonitrile solution reveal the negative and reversible one-electron oxidation, which is typical for aminoferrocenes.^{7c,8b} Introduction of two phenyl substituents at the ferrocenyl moiety makes the oxidation more difficult (**L1**: $E^{0r} = -0.41$ V, **L2**: $E^{0r} = -0.33$ V, vs ferrocene), while the complexation of the rare earth metal only slightly withdraws electron density from the ferrocenyl subunit (**2a**: $E^{0r} = -0.32$ V, vs ferrocene). Even at the slow scan rate of 10 mV/s the oxidation of **2a** remains fully reversible, which indicates that the oxidized complex does not decompose within the minutes time scale.

Single-crystalline material of **2b**·(0.5C₆H₅CH₃) was obtained by slow evaporation of a toluene solution. The molecular structure (Figure 1) features the heterobimetallic iron/rare-earth complex bridged by two Cp-amide moieties. The coordination geometry of the pentacoordinated lutetium center is best described as slightly distorted trigonal-bipyramidal with the oxygen atoms occupying the apical positions (O–Lu–O = 176.17(5)°). A comparison with other pentacoordinated Lu geometries¹¹ reveals that the Lu–N bonds (N1: 2.1839(17) Å, N2: 2.1848(18) Å) and the Lu–O distances (O1: 2.3207(18) Å, O2: 2.2852(16) Å) are relatively short (ranges: Lu–N, 2.18(4)–2.238(3) Å, Lu–O, 2.330(3)–2.346(3) Å). The sums of

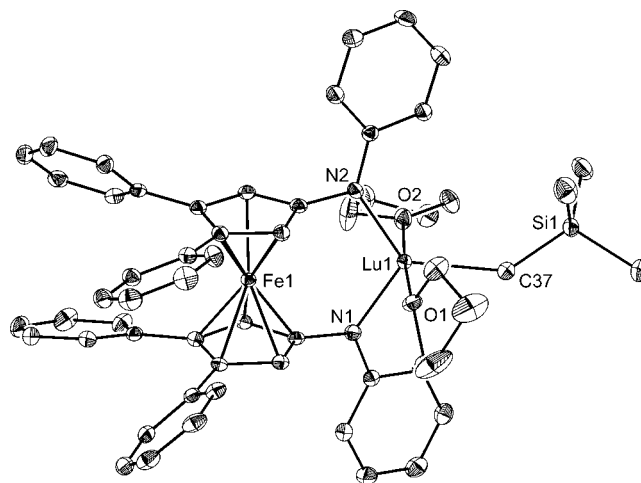


Figure 1. Molecular structure of compound **2b**. Hydrogen atoms and solvent molecule (0.5 toluene per unit cell) are omitted for clarity. Thermal ellipsoids are drawn at the 50% probability level.

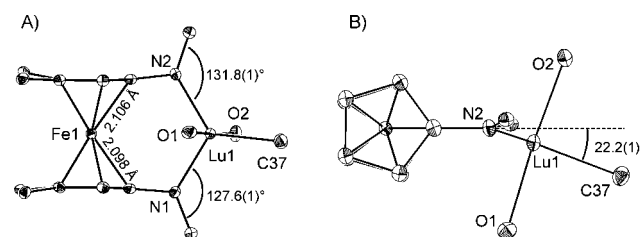


Figure 2. Distortions of the central FcN₂Lu core of **2b**: (A) parallel orientation of paper and N1–C4–C9–N2 plane; (B) orthogonal orientation of paper and N1–C4–C9–N2 plane.

bond angles at both nitrogen atoms (N1: 359.4(4)°, N2: 360.0(4)°) indicate a perfect sp²-hybridization with a slight compression of the C_{Fc}–N–Lu angles (N1: 115.99(12) Å, N2: 113.68(12) Å). Both amide phenyl rings are oriented coplanar with respect to the C_{Fc}–N bonds and orthogonal to the Cp planes. This maximizes the overlap between the filled p-orbital at the nitrogen and the π*-orbitals of the less electron rich adjacent aromatic moieties, which is reflected by a significant shortening of the corresponding C_{Phenyl}–N bonds of 2.4(3) pm with respect to the corresponding C_{Fc}–N bonds. The phenyl substituents at the ferrocenyl backbone are arranged in the expected propeller-type fashion to minimize steric interactions, yet the FcN₂Lu core displays some unexpected distortions (Figure 2). While the two Cp rings and the C–N bonds are virtually coplanar (Cp–Fe–Cp: 179.22(3)°, N1–C4–C9–N2: –1.24(17)°), it is noteworthy that the N1–N2-distance (3.696(7) Å) is significantly larger than the separation of the Cp planes (3.6667(7) Å).

Further, the Lu³⁺ center displays a tilt of 22.2(1)° toward the ferrocenyl group with respect to the plane defined by the two C_{Fc}–N bonds. It might be tempting to attribute these structural distortions to a Lu–Fe interaction, since they cause a decrease of the Fe–Lu distance. However, while the geometric orientation of the lutetium cation is favorable for an interaction with the iron center,¹² the Lu–Fe separation of 3.748(3) Å is 0.76 Å larger than the sum of the metallic radii^{13,14} and hence makes any significant covalent interaction unlikely. Since the arrangement of the molecules in the unit cell gives no evidence for deformations due to packing effects, the distortions described above are best interpreted as a result of the optimized embedding of the Lu³⁺ center in the negatively charged sp² orbitals of the

(10) Avent, A. G.; Cloke, F. G. N.; Elvidge, B. R.; Hitchcock, P. B. *Dalton Trans.* **2004**, 1083–1096.

(11) Anwander, R.; Runte, O.; Eppinger, J.; Gerstberger, G.; Herdtweck, E.; Spiegler, M. *Dalton Trans.* **1998**, 847–858.

Table 1. Results for the MMA Polymerization with the Rare-Earth Alkyl Initiators 1a–3a^a

entry	initiator	yield (%) ^d	10 ⁻³ M _n ^e (g/mol)	M _w /M _n ^e	tacticity <i>rr/rm/mm</i> ^g
1	1a	>98	56.8	9.53 ^f	31/23/46
2	1b	>98	55.8	10.9 ^f	22/29/49
3	2a	>98	476	1.48	19/29/52
4	2b	>98	295	4.38	5/18/77
5	2b^b	>98	47.8	14.29 ^f	33/25/45
6	2b^c	1	n.d.	n.d.	n.d.
7	3a	18	81.7	4.07	30/26/44
8	3a^c	17	30.7	12.5	65/27/8

^a Conditions: toluene/MMA (v/v) = 10/1, MMA/initiator = 500/1, *t* = 6 h at 25 °C. ^b Addition of NBu₄⁺BF₄⁻ after 5 min (1 equiv with respect to initiator). ^c Addition of Fc⁺BF₄⁻ after 5 min (1 equiv with respect to initiator). ^d Determined from amount of material precipitated by addition of MeOH. ^e From GPC relative to PS standards. ^f Bimodal weight distribution. ^g *rr*, *mr*, and *mm* correspond to the percentage of syndio-, hetero-, and isotactic triads.

amide moieties. The steric interaction/ π -stacking of the four phenyl substituents not only locks the Cp rings in an eclipsed conformation, it also prevents any tilting of the Cp rings to adjust the geometry of the diamide pincer accommodating the large rare-earth metal. Thus, the latter is achieved by an elongation of the two Fe–C(N) distances (C4: 2.0977(19) Å, C9: 2.106(2) Å) in comparison to the average of the remaining Fe–C distances (2.071(6) Å) as well as a bending of the C–N bonds against the Cp planes (C4–N1: 4.7(1)°, C9–N2: 7.3(1)°).

The unique spatial assembly of a rare-earth metal in close proximity to a ferrocenyl moiety encouraged us to investigate the influence of the sterically shielding, yet redox-active backbone on the catalytic properties. First studies on the applicability of compounds **1a–2b** as precatalysts for the polymerization of methyl methacrylate (MMA) demonstrated that the diamidoferrocene complexes very efficiently initiate polymer formation (Table 1). MMA is converted quantitatively within 6 h at room temperature, yielding polymers with very high molecular weights even exceeding $M_w = 1.2 \times 10^6$ g/mol in the case of the lutetium complex **2b**. Remarkably, the polymerization properties are mainly determined by the substitution pattern of the ferrocenyl backbone, whereas a change of the metal center is of secondary influence. Complexes of the unsubstituted chelator **L1** yield a broad, bimodal molecular weight distribution, indicating a structurally flexible environment of the active chain end. The high rigidity introduced by the four phenyl groups of **L2** leads to a 5- to 8-fold increase in molecular weight and a substantially reduced polydispersity, which in the case of the yttrium alkyl **2a** (PDI = 1.48) is indicative for a single-site catalytic system. The increase in molecular weights corresponds to an reduced initiator efficiency ($F/\%$ = 88 (**1a**), 90 (**1b**), 10 (**2a**), 17 (**2b**)) for the more rigid systems. Both the activities and molecular weights realized with the ferrocenyl-bridged initiators well exceed those achieved with compound

3a or recently reported results for solution polymerization of MMA with diamido-chelates of lanthanoids.^{5,6} The polymer microstructure as judged by ¹H NMR is predominantly isotactic, with an increasing probability for *mm*-triads with a higher rigidity of the ligand and a decreased size of the metal center.

The proximity of the Fe(II) and the rare-earth metal center triggers a redox sensitization of the alkyl complexes **1a–2b**, which is unveiled upon the addition of ferrocenium salts to a reaction mixture (entry 6). Here, the instant color change to dark red is in marked contrast to polymerizations initiated by the ethylene-bridged compound **3a**, where the solution stays colorless. Despite its low solubility, the ferrocenium salt seems to immediately oxidize the diamidoferrocene ligands, which leads to a rapid termination of the polymerization. In contrast, the addition of NBu₄BF₄ does not change the polymer yields, yet it has a marked effect on the polymer characteristics (entries 5 and 8). Thus, the deactivation of the polymerization catalyst is only experienced for the combination of a ligand with ferrocene backbone and a ferrocenium salt. This is surprising since cyclic voltametric studies indicate a high stability of the oxidized complex.

Conclusion

In conclusion, the introduction of a ferrocenyl backbone into chelates of rare-earth metal alkyls leads to a strongly enhanced complex stability, which is reflected by a higher activity of the complexes when applied as initiators for MMA polymerization. Surprisingly, the polymer properties are mainly influenced by the substitution pattern of the ferrocenyl moiety, which we attribute to changes in the rigidity of the ferrocenyl backbone. The unique orientation of the rare-earth metal and Fe(II) center seems to result in a redox sensitization of the polymerization catalyst. The actual mechanism of the redox-induced termination step will be evaluated in further studies.

Experimental Section

Reagents. Commercially available solvents and reagents were purified according to literature procedures. All reactions were stirred in dry solvents under an argon atmosphere using standard Schlenk and cannula techniques or a conventional glovebox. Y(CH₂SiMe₃)₃(THF)₂, Lu(CH₂SiMe₃)₃(THF)₂,^{6,9} dianilinoferrocene,^{8b,c} bis(1-anilino-3,4-diphenylcyclopentadienyl)iron(II), ArNHCH₂CH₂NHAr (Ar: C₆H₃-¹Pr₂), and ArNHCH₂CH₂NHAr (Ar: C₆H₂-Me₃)¹⁵ were prepared based on published procedures. Methyl methacrylate was dried using a method described previously.¹⁶ All other chemicals were obtained from common suppliers and used without further purification.

Analytical Methods. NMR spectra were recorded at 300 K with a FT-JEOL-JNM-GX-400 (¹H NMR 399.80 MHz, ¹³C NMR 100.52 MHz), a FT-JEOL-JNM-GX-270 (¹H NMR 270.17 MHz, ¹³C NMR 67.93 MHz), or a Bruker DPX 400 (¹H NMR 400.13 MHz, ¹³C NMR 100.61 MHz). ¹H NMR were referenced to the residual ¹H-impurities in the solvent, and ¹³C NMR, to the solvent signal: C₆D₆ (7.15 ppm, 128.0 ppm). GPC analyses: Fa. Waters, HPLC-pump model 510, RI-Detektor model 410, column: PLgel 5 μm Mixed-C (PLgel 5 μm Guard, 50 × 7.5 mm, PLgel 5 μm Mixed-C, 300 × 7.5 μm, PLgel 5 μm Mixed-C, 600 × 7.5 mm), eluent: CHCl₃, flow: 1.0 mL/min, calibration with PS standards

(12) (a) A dative bond to Lewis-acidic metal centers oriented in the mirror plane of the Cp rings has been proposed repeatedly due to the maximum density of the occupied orbitals which correspond to the a'1 and e'2 of an unsubstituted ferrocene, e.g.: Mann, G.; Shelby, Q.; Roy, A. H.; Hartwig, J. F. *Organometallics* **2003**, *22*, 2775–789. (b) van Leeuwen, P. W. N. M.; Zuideveld, M. A.; Swennenhuis, B. H. G.; Freixa, Z.; Kamer, P. C. J.; Goubitz, K.; Fraanje, J.; Lutz, M.; Spek, A. L. *J. Am. Chem. Soc.* **2003**, *125*, 5523–5529. (c) Irigoras, A.; Mercero, J. M.; Silanes, I.; Ugalde, J. M. *J. Am. Chem. Soc.* **2001**, *123*, 5040–5043.

(13) Wells, A. F. *Structural Inorganic Chemistry*, 5th ed.; Oxford University Press: New York, 1984.

(14) (a) Kempe, R.; Noss, H.; Irrgang, T. *J. Organomet. Chem.* **2002**, *647*, 12–20. (b) Costes, J.-P.; Clemente-Juan, J. M.; Dahan, F.; Dumestre, F.; Tuchadues, J.-P. *Inorg. Chem.* **2002**, *41*, 2886–2891. (c) Spannenberg, A.; Oberthür, M.; Noss, H.; Tillack, A.; Arndt, P.; Kempe, R. *Angew. Chem., Int. Ed.* **1998**, *37*, 2079–2082.

(15) (a) Arduengo, A. J., III; Krafczyk, R.; Schmutzler, R.; Craig, H. A.; Goerlich, J. R.; Marshall, W. J.; Unverzagt, M. *Tetrahedron* **1999**, *55*, 14523. (b) Abrams, M. B.; Scott, B. L.; Baker, R. T. *Organometallics* **2000**, *19*, 4944.

(16) Allen, R. D.; Long, T. E.; McGrath, J. E. *Polym. Bull.* **1986**, *15*, 127.

(Polymer Standards Service, molecular weights from $M_n = 1680$ to $M_n = 2.06 \times 10^6$ g/mol). ESI mass spectra: Finnigan MAT 90. Element analyses: Mikroanalytisches Laboratorium der Technischen Universität München. Underestimation of carbon content is common for silicon-containing substances due to carbide formation. Cyclic voltammetry: the standard electrochemical instrumentation consisted of a Princeton Applied Research potentiostat/galvanostat (model 273 A). Cyclic voltammograms were recorded in dry CH_3CN under an argon atmosphere at ambient temperature. A three-electrode configuration was employed. The working electrode was a Pt disk (diameter 1 mm) sealed in soft glass, and the counter electrode, a Pt disk (area 3 cm^2). Solutions were ca. $1 \times 10^{-3} \text{ mol dm}^{-3}$. $(\text{NBu}_4)\text{ClO}_4$ (0.2 M) was used as a supporting electrolyte.

[H₄Fc(NPh)₂]Y(THF)₂CH₂SiMe₃ (1a). In a glovebox Y(CH₂SiMe₃)₃(THF)₂ (165 mg, 0.33 mmol) dissolved in 5 mL of hexane is dropwise added to a solution of dianilinoferrocene (**L1**) (123 mg, 0.33 mmol) in 20 mL of toluene. The reaction solution is stirred for 14 h at room temperature and changes color from red-orange to dark red. The reaction solution is filtered to remove any insoluble contaminations; after this the volatiles are removed under vacuum and the crude product is washed with hexane. Recrystallization from toluene/hexane at -35°C afforded **1a** (179 mg, 79%) as red-orange crystals. ¹H NMR (400 MHz; 25 °C; C₆D₆): δ 7.34–6.67 (m, 10H, Ar-H), 4.18 (s, 4H, Cp-H), 3.65 (br, 8H, THF), 3.39 (s, 4H, Cp-H), 1.05 (br, 8H, THF), 0.53 (s, 9H, Si(CH₃)₃), -0.15 (d, ³J_{H,H} = 3.2 Hz, 2H, CH₂) ppm. ¹³C NMR (100.5 MHz; 25 °C; C₆D₆): δ 157.37, 129.79, 129.28, 125.64 (Ar-C), 115.09, 97.13 (Cp-C), 67.93 (THF), 67.57 (Cp-C), 32.93 (²J_{Y,C} = 40.2 Hz, CH₂), 25.11 (THF), 4.49 (Si(CH₃)₃) ppm. Anal. Calcd for C₃₄H₄₅FeN₂O₂SiY (686.57): C 59.48, H 6.61, N 4.08. Found: C 58.92, H 6.44, N 3.96.

[H₄Fc(NPh)₂]Lu(THF)₂CH₂SiMe₃ (1b). In a glovebox Lu(CH₂SiMe₃)₃(THF)₂ (181 mg, 0.31 mmol) dissolved in 5 mL of hexane is dropwise added to a solution of dianilinoferrocene (**L1**) (115 mg, 0.31 mmol) in 20 mL of toluene. The reaction solution is stirred for 14 h at room temperature and changes color from red-orange to dark red. The reaction solution is filtered to remove any insoluble contaminations; after this the volatiles are removed under vacuum and the crude product is washed with hexane. Recrystallization from toluene/hexane at -35°C afforded **1b** (175 mg, 73%) as red crystals. ¹H NMR (400 MHz; 25 °C; C₆D₆): δ 7.34–6.67 (m, 10H, Ar-H), 4.18 ("t", 4H, Cp-H), 3.70 (br, 8H, THF), 3.41 ("t", 4H, Cp-H), 1.05 (br, 8H, THF), 0.52 (s, 9H, Si(CH₃)₃), -0.33 (s, 2H, CH₂) ppm. ¹³C NMR (100.5 MHz; 25 °C; C₆D₆): δ 157.66, 129.07, 128.28, 127.51 (Ar-C), 114.98, 96.15 (Cp-C), 67.65 (THF), 67.47 (Cp-C), 38.83 (CH₂), 24.71 (THF), 4.36 (Si(CH₃)₃) ppm. Anal. Calcd for C₃₄H₄₅FeN₂O₂SiLu (772.63): C 52.85, H 5.87, N 3.63. Found: C 52.52, H 5.64, N 3.73.

[Ph₄Fc(NPh)₂]Y(THF)₂CH₂SiMe₃ (2a). In a glovebox Y(CH₂SiMe₃)₃(THF)₂ (292 mg, 0.59 mmol) dissolved in 5 mL of hexane is dropwise added to a solution of bis(1-anilino-3,4-diphenylcyclopentadienyl)iron(II) (**L2**) (400 mg, 0.59 mmol) in 40 mL toluene. The reaction solution is stirred for 14 h at room temperature and changes color from red-orange to dark red. The reaction solution is filtered to remove any insoluble contaminations; after this the volatiles are removed under vacuum and the crude product is washed with hexane. Recrystallization from toluene/hexane at -35°C afforded **2a** (450 mg, 83%) as red crystals. ¹H NMR (400 MHz; 25 °C; C₆D₆): δ 7.31–6.70 (m, 30H, Ar-H), 4.35 (s, 4H, Cp-H), 3.86 (br, 8H, THF), 1.13 (br, 8H, THF), 0.45 (s, 9H, Si(CH₃)₃), -0.12 (d, ³J_{H,H} = 3.2 Hz, 2H, CH₂) ppm. ¹³C NMR (100 MHz; 25 °C; C₆D₆): δ 149.66, 135.88, 134.93, 130.32, 130.06, 128.01, 126.62, 126.29, 120.83 (Ar-C), 118.35, 97.79, 86.39 (Cp-C) 67.83 (THF), 25.57 (THF), 25.5 (CH₂), 1.72 (Si(CH₃)₃) ppm. Anal. Calcd. for C₅₈H₆₁FeN₂O₂SiY (990.95): C 70.30, H 6.20, N 2.83. Found: C 70.12, H 5.94, N 2.81.

[Ph₄Fc(NPh)₂]Lu(THF)₂CH₂SiMe₃ (2b). In a glovebox Lu(CH₂SiMe₃)₃(THF)₂ (115 mg, 0.20 mmol) dissolved in 5 mL of hexane

is dropwise added to a solution of bis(1-anilino-3,4-diphenylcyclopentadienyl)iron(II) (**L2**) (134 mg, 0.20 mmol) in 40 mL of toluene. The reaction solution is stirred for 14 h at room temperature and changes color from red-orange to dark red. The reaction solution is filtered to remove any insoluble contaminations; after this the volatiles are removed under vacuum and the crude product is washed with hexane. Recrystallization from toluene/hexane at -35°C afforded **2b** (185 mg, 82%) as dark red crystals. ¹H NMR (270 MHz; 25 °C; C₆D₆): δ 7.32–6.71 (m, 30H, Ar-H), 4.34 (s, 4H, Cp-H), 3.92 (br, 8H, THF), 1.13 (br, 8H, THF), 0.51 (s, 9H, Si(CH₃)₃), -0.32 (s, 2H, CH₂) ppm. ¹³C NMR (67.5 MHz; 25 °C; C₆D₆): δ 157.26, 137.64, 136.51, 129.67, 129.07, 128.31, 126.11, 125.45, 115.40 (Ar-C), 114.98, 99.50, 85.49 (Cp-C), 69.30 (THF), 40.62 (CH₂), 24.96 (THF), 4.28 (Si(CH₃)₃) ppm. Anal. Calcd for C_{61.5}H₆₅FeN₂O₂SiLu (1123.07): C 65.77, H 5.83, N 2.49. Found: C 65.45, H 5.79, N 2.43.

[ArNCH₂CH₂NAr]Y(THF)₂CH₂SiMe₃, Ar = C₆H₃-ⁱPr₂ (3a). In a glovebox Y(CH₂SiMe₃)₃(THF)₂ (114 mg, 0.23 mmol) dissolved in 5 mL of toluene is dropwise added to a solution of ArNHCH₂CH₂NHAr, Ar = C₆H₃-ⁱPr₂ (**L3**) (87.5 mg, 0.23 mmol), in 5 mL of toluene at -25°C . The reaction solution is stirred for 14 h at room temperature and changes color from pale yellow to orange. The reaction solution is filtered to remove any insoluble contaminations; after this the volatiles are removed under vacuum and the crude product is redissolved in hexane. Recrystallization from hexane at -35°C afforded **3a** (101 mg, 63%) as orange crystals. ¹H NMR (400 MHz; 25 °C; C₆D₆): δ 7.23–7.21 (d, 4H, Ar-H), 7.12–7.10 (t, 2H, Ar-H), 4.29–4.19 (sep, 4H, CH(CH₃)₂), 4.05 (s, 4H, CH₂), 3.31 (br, 8H, THF), 1.40 (s, 24H, CH₃), 1.02 (br, 8H, THF), 0.37 (s, 9H, Si(CH₃)₃), -0.41 (d, ³J_{H,H} = 3.7 Hz, 2H, CH₂) ppm. ¹³C NMR (100.6 MHz; 25 °C; C₆D₆): δ 155.25, 145.32, 123.15, 121.75 (Ar-C), 69.50 (THF), 59.52 (N-CH₂), 27.93 (CH₃), 26.02 (CH(CH₃)₂), 25.56 (Y-CH₂), 24.62 (THF), 4.46 (Si(CH₃)₃) ppm. Anal. Calcd for C₃₈H₆₅N₂O₂SiY (698.93): C 65.30, H 9.37, N 4.01. Found: C 64.82, H 9.04, N 3.83.

[ArNCH₂CH₂NAr]Lu(THF)₂CH₂SiMe₃, Ar = C₆H₃-ⁱPr₂ (3b). In a glovebox Lu(CH₂SiMe₃)₃(THF)₂ (132 mg, 0.23 mmol) dissolved in 5 mL of toluene is dropwise added to a solution of ArNHCH₂CH₂NHAr, Ar = C₆H₃-ⁱPr₂ (**L3**) (87.5 mg, 0.23 mmol), in 5 mL toluene at -25°C . The reaction solution is stirred for 14 h at room temperature and changes color from pale yellow to orange. The reaction solution is filtered to remove any insoluble contaminations; after this the volatiles are removed under vacuum. The crude product decomposes rapidly in solution.

[ArNCH₂CH₂NAr]Y(THF)₂CH₂SiMe₃, Ar = Mes (4a). In a glovebox Y(CH₂SiMe₃)₃(THF)₂ (114 mg, 0.23 mmol) dissolved in 5 mL of toluene is dropwise added to a solution of ArNHCH₂CH₂NHAr, Ar = Mes (**L4**) (67.7 mg, 0.23 mmol), in 5 mL of toluene at -25°C . The reaction solution is stirred for 14 h at room temperature and changes color from pale yellow to orange. The reaction solution is filtered to remove any insoluble contaminations; after this the volatiles are removed under vacuum. The crude product decomposes rapidly in solution.

[ArNCH₂CH₂NAr]Y(THF)₂CH₂SiMe₃, Ar = Mes (4b). In a glovebox Lu(CH₂SiMe₃)₃(THF)₂ (132 mg, 0.23 mmol) dissolved in 5 mL of toluene is dropwise added to a solution of ArNHCH₂CH₂NHAr, Ar = Mes (**L4**) (67.7 mg, 0.23 mmol), in 5 mL toluene at -25°C . The reaction solution is stirred for 14 h at room temperature and changes color from pale yellow to orange. The reaction solution is filtered to remove any insoluble contaminations; after this the volatiles are removed under vacuum. The crude product decomposes rapidly in solution.

[PhNCH₂CH₂NPh]Y(THF)₂CH₂SiMe₃ (5a). In a glovebox Y(CH₂SiMe₃)₃(THF)₂ (114 mg, 0.23 mmol) dissolved in 5 mL of toluene is dropwise added to a solution of PhNHCH₂-CH₂NPh (**L5**) (48.5 mg, 0.23 mmol) in 5 mL of toluene at -25 °C. The reaction solution is stirred for 14 h at room temperature and changes color from pale yellow to orange. The reaction solution is filtered to remove any insoluble contaminations; after this the volatiles are removed under vacuum. The crude product decomposes rapidly in solution.

[PhNCH₂CH₂NPh]Lu(THF)₂CH₂SiMe₃ (5b). In a glovebox Lu(CH₂SiMe₃)₃(THF)₂ (132 mg, 0.23 mmol) dissolved in 5 mL of toluene is dropwise added to a solution of PhNHCH₂-CH₂NPh (**L5**) (48.5 mg, 0.23 mmol) in 5 mL of toluene at -25 °C. The reaction solution is stirred for 14 h at room temperature and changes color from pale yellow to orange. The reaction solution is filtered to remove any insoluble contaminations; after this the volatiles are removed under vacuum. The crude product decomposes rapidly in solution.

General Procedure for the Polymerization of Methylmethacrylate (MMA). In a glovebox each lanthanoid-alkyldiamide complex (0.2 mol %) is dissolved in 18 mL of toluene. The solution is stirred at room temperature for 5 min, then 2 mL (18.7 mmol) of methylmethacrylate is rapidly added. The reaction solutions are stirred for the mentioned time. The sometimes very viscous reaction solutions are poured into 100 mL of methanol outside the glovebox. The precipitating polymers are filtered off, dried, and analyzed (mass, GPC analyses, NMR spectroscopy). The methanol solutions are evaporated under vacuum, and the residues are also analyzed via mass spectroscopy.

Acknowledgment. We thank the Stifterverband für die Deutsche Wissenschaft (Projekt-Nr. 11047: ForschungsDozentur Molekulare Katalyse), the Elitenetzwerk Bayern (Fellowship K.N.), and the IDK NanoCat for generous support. We are grateful to Prof. O. Nuyken and his co-workers for

Table 2. Experimental Data for the Crystal Structure Determination of the Complex 2b

empirical formula	C _{61.50} H ₆₅ FeLuN ₂ O ₂ Si
<i>M_r</i>	1123.07
cryst size/mm	0.30 × 0.30 × 0.30
cryst syst	triclinic
space group	<i>P</i> $\bar{1}$
<i>a</i> /Å	12.447(3)
<i>b</i> /Å	15.072(4)
<i>c</i> /Å	15.120(4)
α /deg	69.439(4)
β /deg	76.291(4)
γ /deg	78.331(4)
<i>V</i> /Å ³	2558.1(11)
<i>Z</i>	2
ρ_{calc} /g cm ⁻³	1.458
μ (Mo K α)/mm ⁻¹	2.271
<i>F</i> (000)	1150
<i>T</i> /K	100(2)
θ range/deg	1.46–28.24
no. of reflns collected	25 256
no. of reflns obsd [<i>I</i> > 2 σ (<i>I</i>)]	11 436
no. of indep reflns (<i>R</i> _{int})	11 436 (0.0214)
no. of data/restraints/params	11 436/0/586
GOF	1.046
final <i>R</i> indices <i>R</i> 1 ^a , w <i>R</i> 2 ^b (obsd data)	0.0234, 0.0607
final <i>R</i> indices <i>R</i> 1, w <i>R</i> 2 (all data)	0.0247, 0.0613
largest <i>e</i> (max), <i>e</i> (min)/e Å ⁻³	1.331 and -0.724

$$^a R1(F) = \frac{\sum \Delta F_o}{\sum F_o} \quad \Delta F_c \Delta / \sum F_o. \quad ^b wR2(F) = \frac{[\sum w(F_o^2 - F_c^2)^2 / \sum w(F_o^2)^2]^{1/2}}$$

polymer analysis and helpful discussions. We thank Prof. H.-J. Krüger and his co-workers for cyclovoltammetric measurements.

Supporting Information Available: ¹H NMR spectra for compounds **1a–3a**, cyclovoltamograms of compound **L2** and **2a** as well as crystallographic data for compound **2b** (see also CCDC data depository: 648448) are available free of charge via the Internet at <http://pubs.acs.org>.

OM700988N